
Research Article

Characterising Drug Release from Immediate-Release Formulations of a Poorly Soluble Compound, Basmisanil, Through Absorption Modelling and Dissolution Testing

Cordula Stillhart,^{1,5} Neil J. Parrott,² Marc Lindenberg,³ Pascal Chalus,³ Darren Bentley,⁴ and Anikó Szepes¹

Received 14 January 2017; accepted 10 February 2017; published online 24 February 2017

Abstract. The study aimed to characterise the mechanism of release and absorption of Basmisanil, a biopharmaceutics classification system (BCS) class 2 compound, from immediate-release formulations *via* mechanistic absorption modelling, dissolution testing, and Raman imaging. An oral absorption model was developed in GastroPlus® and verified with single-dose pharmacokinetic data in humans. The properties and drug release behaviour of different oral Basmisanil formulations were characterised *via* biorelevant dissolution and Raman imaging studies. Finally, an *in vitro-in vivo* correlation (IVIVC) model was developed using conventional and mechanistic deconvolution methods for comparison. The GastroPlus model accurately simulated oral Basmisanil exposure from tablets and granules formulations containing micronized drug. Absorption of oral doses below 200 mg was mostly dissolution rate-limited and thus particularly sensitive to formulation properties. Indeed, reduced exposure was observed for a 120-mg film-coated tablet and the slower dissolution rate measured in biorelevant media was attributed to differences in drug load. This hypothesis was confirmed when Raman imaging showed that the percolation threshold was exceeded in this formulation. This biorelevant dissolution method clearly differentiated between the formulations and was used to develop a robust IVIVC model. The study demonstrates the applicability and impact of mechanistic absorption modelling and biopharmaceutical *in vitro* tools for rational drug development.

KEY WORDS: absorption modelling; GastroPlus; immediate-release formulation; *in vitro-in vivo* correlation; poorly water-soluble compound.

INTRODUCTION

The biopharmaceutical behaviour of orally administered compounds is a key property that needs to be considered for the development of novel medicines. Understanding the mechanism of drug release and absorption from an oral formulation improves the prediction of drug bioavailability

Electronic supplementary material The online version of this article (doi:10.1208/s12248-017-0060-1) contains supplementary material, which is available to authorized users.

¹ Formulation Research & Development, F. Hoffmann-La Roche Ltd., Basel, Switzerland.

² Pharmaceutical Research & Early Development, Roche Innovation Center Basel, F. Hoffmann-La Roche Ltd., Basel, Switzerland.

³ Analytical Development, F. Hoffmann-La Roche Ltd., Basel, Switzerland.

⁴ Clinical Pharmacology, F. Hoffmann-La Roche Ltd., Basel, Switzerland.

⁵ To whom correspondence should be addressed. (e-mail: cordula.stillhart@roche.com)

and allows development of safe and effective drug products. This is an important element of the Quality by Design (QbD) strategy for formulation development in the pharmaceutical industry (1). Implementing QbD in pharmaceutical development requires a profound understanding of critical quality attributes and process parameters, as well as the possibility to predict *in vivo* performance based on *in vitro* observations. Establishing this link between formulation properties and *in vivo* performance is, however, often a major challenge.

In vitro dissolution testing is a key biopharmaceutical tool for formulation characterisation. Dissolution profiles are generally used as control parameters for the quality attributes of a drug product, but can also be a surrogate of *in vivo* drug release if an *in vitro-in vivo* correlation (IVIVC) has been established. IVIVC not only provides an opportunity to address post-approval changes, but is also becoming increasingly important at earlier stages of development, for example to estimate the possible impact of changes in formulation composition or manufacturing process on *in vivo* drug release (2). While IVIVC is being routinely used for modified release formulations (2–6), it is much less frequently reported for immediate-release formulations.

Biopharmaceutical modelling and simulation has been recognised as another important tool for establishing the link between drug and formulation properties and *in vivo* performance (7–9). Physiologically based pharmacokinetic (PBPK) models describe the kinetic processes of drug absorption, distribution, metabolism, and excretion considering anatomy and physiology as well as physicochemical properties of drug substance and formulation. Such models can provide information about *in vivo* drug and formulation behaviour, including for example the kinetics of drug dissolution, precipitation, and absorption (8,10,11). Several publications have presented the use of PBPK modelling to understand absorption, with the majority targeting human dose or food effect predictions and only a few specifically focused on formulation properties (9). There is a clear need for more case studies to demonstrate the validity and applicability of biopharmaceutical *in vitro* and *in silico* tools to support their potential, not only for risk assessment and decision making during development but also in a regulatory environment (12).

The current study presents the use of mechanistic absorption modelling and *in vitro* dissolution testing to study the key biopharmaceutical properties of Basmisanil, a selective orally active γ -amino butyric acid (GABA)-A α 5 receptor inverse antagonist which is currently in clinical development. Basmisanil is a low molecular weight molecule exhibiting poor aqueous solubility and good membrane permeability. It was classified as class 2 according to the biopharmaceutics classification system (BCS). Two oral immediate-release formulations were developed, a tablet and a granules in sachet formulation, which contained micronised drug and were similar with respect to the qualitative composition. The formulations were produced using the same manufacturing technology. However, despite these similarities, a single-dose comparative bioavailability study in healthy adult volunteers showed different oral exposure profiles for the two dosage forms.

In the present study, we applied oral absorption modelling using the commercial PBPK software package GastroPlus® and biorelevant *in vitro* dissolution testing to characterise the mechanism of drug release and the root cause for different exposure after oral administration of the formulations. Furthermore, the development of an IVIVC model using different deconvolution methods is presented here, which can be used as a tool for the prediction of oral absorption profiles for future formulation changes.

MATERIALS AND METHODS

API and Formulation Properties

Basmisanil is a lipophilic substance exhibiting poor solubility in aqueous media across the physiological range from pH 1 to pH 9. The physicochemical properties of the drug substance are listed in Table I. Basmisanil was formulated in micronised form and exhibited a D90 of less than 10 μ m.

Three different formulations were developed for clinical studies, as summarised in Table II. Single and multiple ascending dose (SAD and MAD, respectively) studies were conducted with an uncoated, immediate-release tablet formulation exhibiting four different dose strengths (0.5, 5, 40, and

Table I. Physicochemical Characteristics and Kinetics of Disposition of Basmisanil

Parameter	Value
Molecular weight	445.5 g/mol
pK _a	2.07 (base)
logD (pH 7.4)	1.86
Blood/plasma concentration ratio	0.59
Fraction of drug unbound in plasma	5.6%
Solubility	
Aqueous buffer pH 1–9	0.001 mg/mL
SGF pH 1.6	0.008 mg/mL
FaSSIF pH 6.5	0.010 mg/mL
FeSSIF pH 5	0.032 mg/mL
Particle size distribution	
D10	1.4 μ m
D50	4.7 μ m
D90	10.1 μ m
Disposition model parameters	
k ₁₂	1.294 1/h
k ₂₁	0.979 1/h
k ₁₀	0.245 1/h
V _c /kg	0.235 L/kg
V ₂ /kg	0.311 L/kg
CL/kg	0.058 L/h/kg
CL ₂ /kg	0.304 L/h/kg
Elimination half-life	7.0 h

pKa acid dissociation constant, *logD* distribution coefficient, *SGF* simulated gastric fluid, *FaSSIF* fasted state simulated intestinal fluid, *FeSSIF* fed state simulated intestinal fluid, *k*₁₂ and *k*₂₁ transfer rate constant from the central to the peripheral compartment and from the peripheral to the central compartment, respectively, *k*₁₀ elimination rate constant, *V*_c and *V*₂ volumes of distribution of the central compartment and in the elimination phase, respectively, *CL* and *CL*₂ clearances of the central compartment and in the elimination phase, respectively

250 mg). In a second step, a comparative bioavailability study was done using a film-coated tablet and a granules in sachet formulation, both exhibiting a dose strength of 120 mg. The formulations were composed from standard compendial excipients, including α -lactose monohydrate and microcrystalline cellulose as fillers (60–82% *w/w*), polyvinylpyrrolidone as a solid binder (5–6% *w/w*), croscarmellose sodium as a disintegrant (3–4% *w/w*), and magnesium stearate as a lubricant (0.6–1% *w/w*). The tablet and film-coated tablet formulations contained a glidant (2% *w/w* talc) in the extragranular phase. Moreover, an anionic surfactant (1% *w/w* sodium laurylsulfate) was included in the tablet formulation used in SAD studies. However, it was shown to have no significant impact on drug release and was later removed from the film-coated tablet and the granules in sachet formulation. The above-mentioned formulations differed in drug load. The API content of the uncoated tablets ranged between 0.07 and 33.3% *w/w*, while the drug load of the film-coated tablet and the granules in sachet formulation was 26.7% *w/w* and 12.8% *w/w*, respectively (Table II).

The granules were produced *via* roll compaction and then filled into sachets or compressed into biconvex-shaped tablets after addition of filler, glidant, and lubricant in the extragranular phase. The compaction blend was prepared *via* mixing the API stepwise with the excipients of the

Table II. Overview of Oral Formulations

Formulation type	Dose strength (mg/unit)	Weight of dosage form (mg/unit)	Drug load (% w/w)	Clinical study
Uncoated tablet	0.5	750	0.07	SAD/MAD
	5	750	0.7	
	40	750	5.3	
	250	750	33.3	
Film-coated tablet	120	450 ^a	26.7	Comparative bioavailability study
Granules in stick-pack formulation	120	936 ^b	12.8	

SAD/MAD single and multiple ascending dose studies

^aWeight of uncoated tablet core

^bFill weight of stick pack

intragranular phase in order to achieve homogeneous blends. Film-coating was performed using a rapidly dissolving film-coat based on hydroxypropylmethylcellulose.

Pharmacokinetics of Basmisanil in Healthy Adults

The pharmacokinetic profile of Basmisanil was determined after intravenous and peroral administration in six healthy adult volunteers. An intravenous microdose of 0.1 mg [¹³C]-labelled API was administered as an aqueous solution by a constant rate infusion over 15 min, starting 3.75 h after the administration of an oral dose of 160 mg. Plasma concentrations were measured pre-dose, as well as 5, 15, 20, 25, 30, 45 min, and 2.25, 4.25, and 8.25 h post-dose.

In SAD and MAD studies, single doses of between 1.5 and 1250 mg were administered to six healthy adults per dose level. The tablets (dose strength 0.5, 5, 40, or 250 mg, Table II) were given with 250 mL of still water within 5 min after completion of a standardised meal. Plasma concentrations of Basmisanil were measured pre-dose, as well as 0.5, 1, 1.5, 2, 2.5, 3, 4, 6, 8, 11, 14, 24, 36, 48, and 72 h post-dose.

The single-dose comparative bioavailability study, which compared the pharmacokinetic performance of the 120-mg film-coated tablet and the 120-mg granules in sachet formulations, was a randomised cross-over study in 18 healthy adult volunteers. Single doses were administered orally within 30 min of the start of a standard high-fat, high-calorie breakfast. Film-coated tablets were swallowed whole with 240 mL of still water. Granules in sachet were mixed with or sprinkled onto a tablespoon of apple sauce and the whole mixture was swallowed followed by 240 mL of still water. There was a 4-day washout period between study drug administrations (film-coated tablet or granules in sachet formulation). Plasma concentrations of Basmisanil were determined pre-dose, as well as 0.5, 1, 1.5, 2, 3, 4, 5, 6, 8, 10, 12, 16, 24, 36, 48, and 60 h post-dose. All clinical studies were reviewed and approved by independent ethics committees (North London Research Ethics Committee, London, UK; Stichting Beoordeling Ethiek Bio-Medisch Onderzoek, Assen, NL; National Research Ethics Service Committee North East—York, Jarrow, UK).

Simulation of Plasma Concentration Profiles Following Oral Administration

The disposition kinetics of Basmisanil was described using a two-compartment PK model fitted to the mean plasma

concentration-time profile obtained after a single intravenous administration of 0.1 mg [¹³C]-labelled drug to six healthy male volunteers. The model fitting was performed in the PKPlus® module of GastroPlus and the derived pharmacokinetic parameters were integrated in the GastroPlus model together with the physicochemical and physiological parameter values (Table I). *In vivo* drug release was predicted using the Johnson dissolution model (13) and immediate-release kinetics was assumed for all formulations (“IR tablet” for uncoated and film-coated tablets; “IR suspension” for the sachet formulation). The drug particle size distribution was included (Table I) and it was assumed that particles were distributed into three bins with constant radii. Drug solubility was determined experimentally in simulated gastric fluid (SGF) pH 1.6, fasted state simulated intestinal fluid (FaSSIF) pH 6.5, and fed state simulated intestinal fluid (FeSSIF) pH 5.0 at 37°C (14). The effective human jejunal permeability of 3.75×10^{-4} cm/s was obtained from permeability measurement across Caco-2 cells. The conversion of *in vitro* permeability to an estimate of human jejunal permeability was done as described previously (15). Due to the very low extraction ratio of <5% of the liver blood flow, no first pass extraction was assumed in the oral absorption model. We simulated plasma concentration-time profiles for oral doses from 1.5 to 1250 mg Basmisanil under fed state conditions by using the “Human-Physiological-Fed” physiology and the default absorption scale factor model (Opt logD Model SA/V 6.1). An overview of clinical data used for oral absorption modelling is reported in the [Supplementary Material](#).

Parameter Sensitivity Analysis

A parameter sensitivity analysis (PSA) was conducted to explore the sensitivity of rate and extent of oral absorption (expressed as peak plasma concentration, C_{max} , and fraction absorbed, F_a , respectively) to the mean drug particle radius. The mean drug particle radius was varied in the range of 0.5 to 50 μ m with logarithmic spacing (10 tests) for 1.5, 120, and 330 mg doses in the fed state.

In Vitro Dissolution Testing

In vitro dissolution of the tablets, film-coated tablet, and granules in sachet formulation (Table II) was tested using a United States Pharmacopoeia (USP) type 2 dissolution apparatus in 900 mL FeSSIF medium (14) at 37°C. The rotation speed was set to 50 rpm. Fractions of the

formulations containing a constant amount of drug (40 mg) were tested. Samples were removed after 5, 15, 30, 45, 60, 90, and 120 min, filtered, and analysed *via* high performance liquid chromatography (HPLC) with UV detector. Dissolution experiments were conducted in triplicate.

Raman Imaging

Raman imaging of 40 mg tablet, 120 mg film-coated tablet, and 120 mg granules in sachet formulations was performed using a Renishaw InVia Streamline microscope (Renishaw plc, Wotton-under-Edge, UK). To obtain a flat surface of the sample, the tablets were cut in their length using a Leica EM Trim specimen trimming device (Leica, Wetzlar, Germany). For data acquisition, the $\times 20$ objective was used. The excitation wavelength of the laser source was 785 nm. The optical bench was set to use a 1200 l/mm grating, allowing spectral acquisition between 555 and 1676 cm^{-1} Raman shifts with a resolution of 1 cm^{-1} . The exposure time was 0.44 s using a binning of three pixels on the detector resulting in a spatial resolution of 21.3 μm per pixel. The image size was approx. 150×150 pixels, resulting in 22'500 spectra per image of approx. 3×3 mm size.

The false colour images were recalculated using the direct classical least squares (DCLS) analysis algorithm in WiRE[®] 4.1 (Renishaw plc, Wotton-under-Edge, UK), given the pure spectra of the API and the excipients.

IVIVC Model Development

IVIVC modelling was conducted using the IVIVCPlus[®] module in GastroPlus version 9.0. First, an IVIVC model was developed with a limited number of datasets, i.e. those obtained from the single-dose PK study, where the 120-mg film-coated tablet and the 120-mg sachet formulation were tested. Three different deconvolution methods to obtain an *in vivo* dissolution profile were compared: the two-compartment Loo-Riegelmann method (16), the numerical deconvolution method (17), and the GastroPlus Mechanistic Absorption model (18). For the numerical and the GastroPlus Mechanistic Absorption method, the deconvoluted *in vivo* dissolution profiles were fitted using a single and a double Weibull function for comparison. The deconvoluted *in vivo* dissolution profiles were then correlated to the *in vitro* dissolution data in FeSSIF pH 5 for each specific formulation. The best correlation function was selected based on the Akaike Information Criterion (AIC). The model predictability was evaluated for each deconvolution method in terms of correlation coefficient (R^2), standard error of prediction (SEP), mean absolute error (MAE), and AIC. External model validation was finally done with *in vivo* data obtained from SAD and MAD studies.

RESULTS

Pharmacokinetic Profiles Following Oral Drug Administration

The mean plasma concentration-time profiles following single administrations of 1.5 to 1250 mg Basmisanil in the fed state are shown in Fig. 1a (six subjects per dose). The drug

was administered as an uncoated tablet formulation exhibiting dose strengths of 0.5, 5, 40, and 250 mg in these studies. Basmisanil was rapidly absorbed with maximum plasma concentrations (C_{max}) observed at approximately 4 h (T_{max}) although some prolongation was apparent at higher doses. C_{max} increased in a dose-proportional manner for doses up to 160 mg, and in a less than proportional manner thereafter. The same trend was observed with $\text{AUC}_{0\text{-last}}$.

In the single-dose comparative bioavailability study, the oral exposure following administration of a 120-mg film-coated tablet and a 120-mg granules formulation was determined in 18 adults in the fed state. As shown by the plasma concentration-time profiles in Fig. 1b, significantly different exposures were observed for the two formulations, despite their similarity in qualitative composition and the same applied granulation process. The exposure from the granules formulation was higher than from the film-coated tablet, resulting in a C_{max} of 1.6 and 1.2 $\mu\text{g}/\text{mL}$ and $\text{AUC}_{0\text{-inf}}$ of 23.0 and 17.5 $\mu\text{g}\cdot\text{h}/\text{mL}$ for granules and film-coated tablet, respectively.

GastroPlus Modelling of Uncoated Tablet Study Data

GastroPlus simulations were conducted for the oral plasma concentration-time profiles depicted in Fig. 1a, b. We assumed immediate drug release using the Johnson dissolution model, while the drug disposition parameters obtained from two-compartment model fitting were kept constant. The model captured the dose proportionality observed in exposure from uncoated tablet dosing over a dose range from 1.5 to 1250 mg (tablet formulation), as shown in Fig. 2. While the prediction of C_{max} was excellent over the entire dose range, AUC was slightly overpredicted especially at lower doses. However, both observed and predicted values showed a clear drop in C_{max} and AUC at doses higher than approximately 160 mg. The overprediction of AUC in the dose range <100 mg was due to more rapid elimination at these doses compared to the 160-mg dose at which disposition kinetics were determined.

A sensitivity analysis for drug particle radius was conducted assuming immediate release from a tablet formulation. Three oral doses were simulated (1.5, 120, and 330 mg) in order to study the parameter sensitivity below, close to, and above the dose threshold of dose-linear pharmacokinetics, respectively. As seen in Fig. 3, drug particle radius had a significant impact on C_{max} and Fa. Also, the effect was strongly dose dependent. For the lowest dose of 1.5 mg, a critical particle radius was found at approximately 5 μm , whereas for the 120 and 330 mg doses, this value was significantly smaller (approx. 2.5 and <1 μm , respectively).

In the GastroPlus model, we assumed that API particles were distributed into three bins with constant particle radius in each bin (1.4, 4.7, and 10.1 μm , respectively). The three bins corresponded to the measured D10, D50, and D90 values of clinical API batches. Increasing the number of bins had no significant impact on the simulation results. The simulated dissolution rate of drug particles belonging to bin 1, bin 2, and bin 3 in the gastrointestinal lumen, following oral administration of 1.5, 120, and 330 mg Basmisanil, is reported in the [Supplementary Materials](#). When simulating the 1.5-mg dose, complete drug dissolution occurred within the small intestine

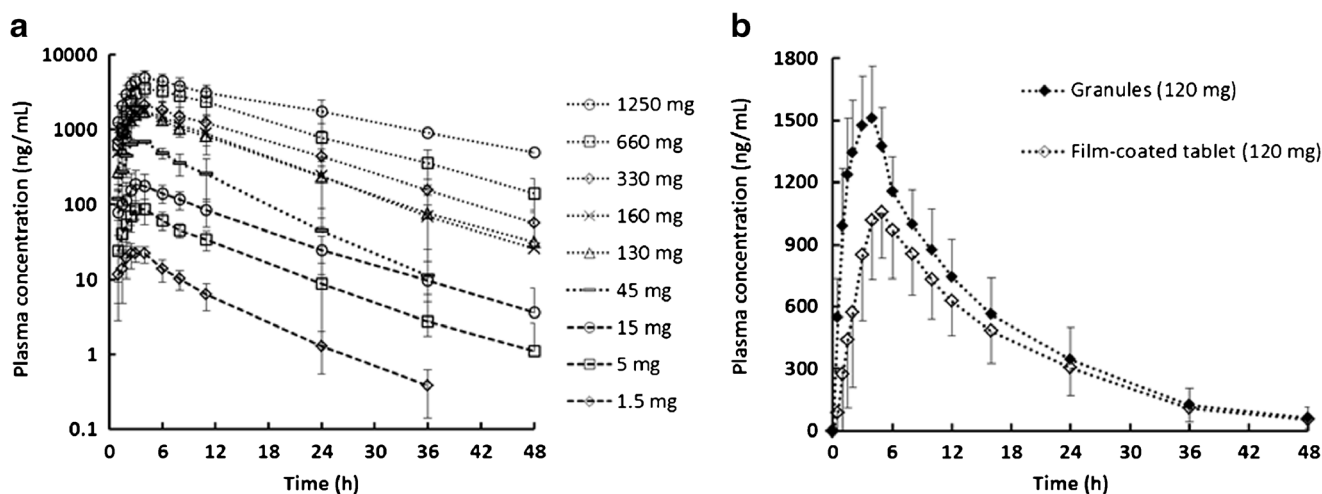


Fig. 1. Mean observed plasma concentration-time profiles following oral administration of **a** tablet formulations and **b** granules and film-coated tablet formulations to healthy adult subjects in the fed state

transit time despite the slightly slower dissolution of larger particles. In contrast, for the 330-mg dose, the % dissolved profile was comparatively low. Only the smallest particles (bin 1) dissolved completely, while particles in bin 2 and bin 3 resulted in incomplete dissolution within the small intestine transit time. Also, a clear drop in dissolution rate was observed after approximately 5 h. The simulated concentration vs. time profiles of Basimisanil in different regions of the intestinal lumen ([Supplementary Material](#)) showed that, with the 1.5-mg dose, the intraluminal concentration was significantly smaller than the predicted solubility measured in FeSSIF media. In contrast, following administration of 120 and 330 mg Basimisanil, the solubility limit was reached in the duodenum and the jejunum.

GastroPlus Modelling of Granules and Film-Coated Tablet Formulations

In a second step, we studied the *in vivo* performance of two different formulations, *i.e.* the 120-mg granules in sachet and the 120-mg film-coated tablet formulation. As shown in Fig. 4a, the GastroPlus model accurately predicted the oral

exposure of the granules in sachet formulation. However, the result was comparatively poor for the film-coated tablet formulation. The model significantly overpredicted the plasma concentrations, resulting in much higher than observed C_{max} and AUC (Fig. 4b). The root cause for the comparatively low exposure with the film-coated tablet formulation was further investigated *via* dissolution testing and Raman spectroscopy.

In Vitro Dissolution Kinetics

The kinetics of drug dissolution from the film-coated tablet and the granules in sachet formulations was measured in FeSSIF pH 5.0. A constant dose-to-volume ratio of 40 mg Basimisanil in 900 mL dissolution medium was kept for each formulation, which corresponded to 120% of the equilibrium solubility of Basimisanil in FeSSIF pH 5.0. Accordingly, only fragments of the film-coated tablets and a defined proportion of the granules were used.

The dissolution curves for the two formulations are presented in Fig. 5. In addition, the dissolution profile of the granules used for tablet compression and those of the final

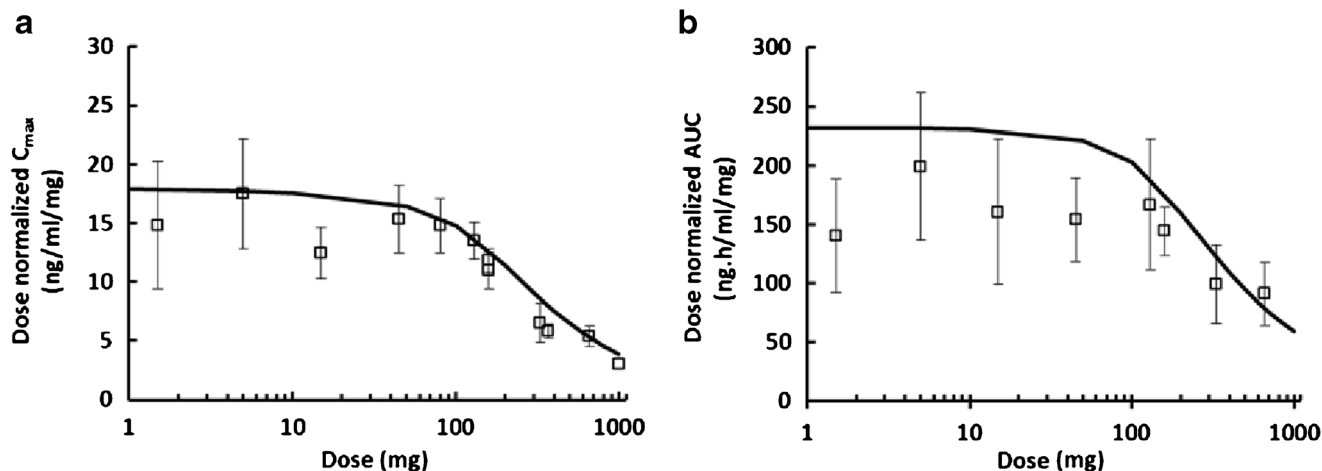


Fig. 2. Mean observed (*empty square*, \pm standard deviation) and simulated (*continuous line*) dose normalised C_{max} (**a**) and AUC (**b**) values obtained from uncoated tablet studies

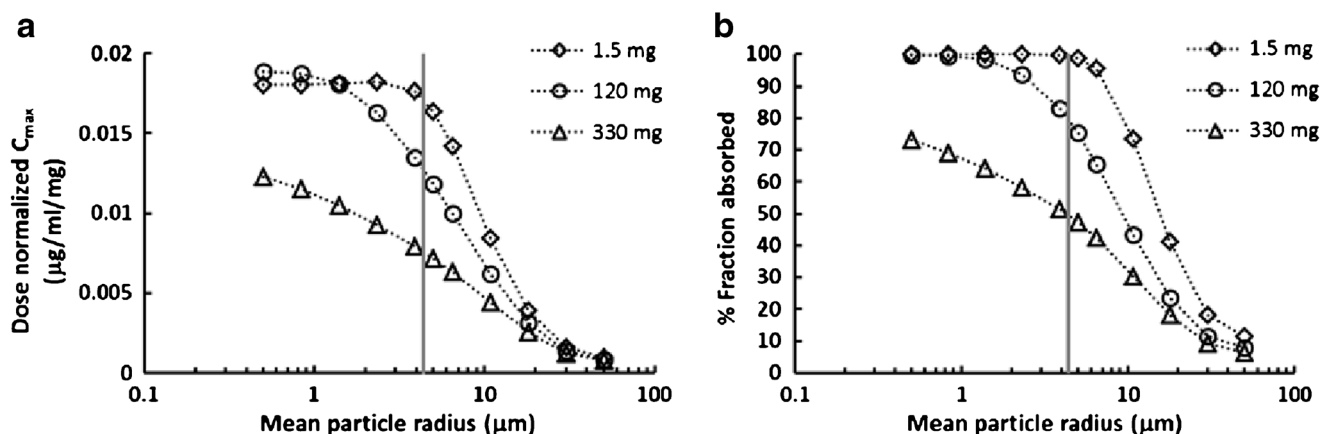


Fig. 3. Simulated impact of drug particle radius on **a** C_{\max} and **b** the fraction absorbed following oral administration of 1.5, 120, and 330 mg Basmisanil. The *grey line* shows the mean drug particle radius of Basmisanil administered in clinical studies

tablet blend containing the extragranular phase were determined. The granules for sachet formulation exhibited the fastest dissolution, reaching the solubility limit in FeSSIF within 45 min. Dissolution from the film-coated tablet formulation was significantly slower and only about 50% of the incorporated drug substance dissolved within 120 min. The granules intended for tablet compression and the final tableting blend showed faster dissolution profiles than the film-coated tablet. It was confirmed in a separate experiment that the film-coating did not have significant influence on the dissolution behaviour under simulated gastric and intestinal conditions (data are not presented here).

Raman Imaging of Basmisanil Formulations

Raman images in Fig. 6 show the distribution of API in the formulation matrix of the 40-mg tablet, the 120-mg film-coated tablet, and the 120-mg granules in sachet formulation. All formulations exhibited areas with high drug particle density, which suggested that the API had cohesive properties in the excipients mixture. This effect was even more pronounced following tablet compression and can be observed when comparing the images of the two tablets and the granules formulation.

A major difference however existed between the 120-mg film-coated tablet and the other two formulations. The 120-mg film-coated tablet showed large agglomerated clusters, in which the drug particles formed a coherent network in the tablet matrix. The other two formulations showed API-rich regions as well, but excipients were still detected within these regions (visible as black shaded regions in Raman images). It can therefore be assumed that the combination of cohesive properties of the micronized API, the compression pressure during tableting, and the high drug load in the tablet formulation resulted in the formation of a coherent API network in the tablet matrix of the 120 mg film-coated tablet.

IVIVC Model

An IVIVC model was developed using *in vitro* dissolution and *in vivo* plasma concentration-time profiles for the 120-mg granules and the 120-mg film-coated tablet formulations. The AIC suggested that the best IVIVC was obtained using the GastroPlus Mechanistic Absorption model to deconvolute *in vivo* data and the single Weibull function to fit the *in vitro* dissolution profiles. The correlation between *in vitro* and *in vivo* data was best described by a power function resulting in an R^2 value of 0.990 (Fig. 7). In contrast,

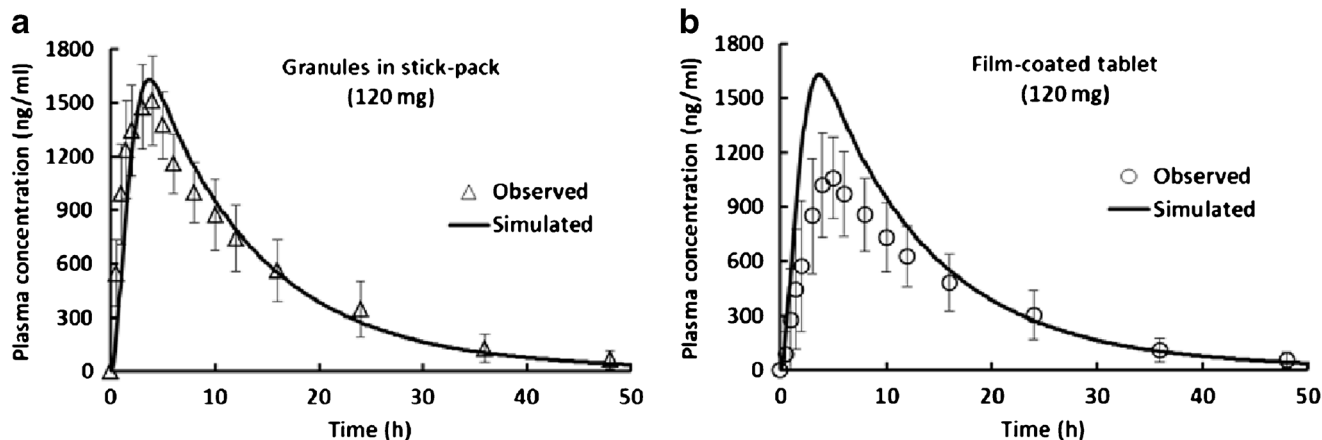


Fig. 4. Observed and simulated plasma concentration-time profiles following oral administration of **a** 120 mg granules in sachet and **b** 120 mg film-coated tablet formulation. Observed data represent mean values and standard deviations ($n = 18$)

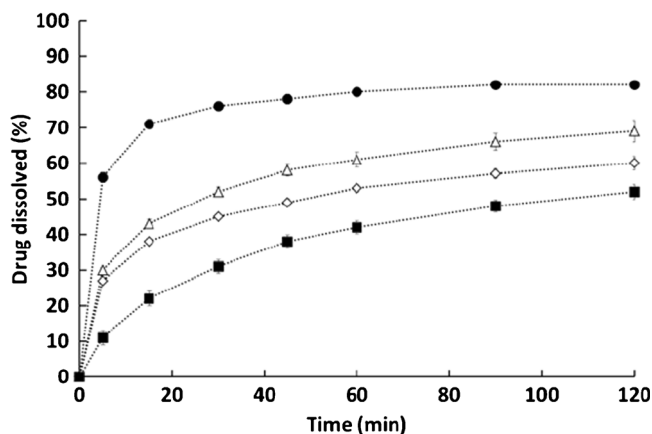


Fig. 5. Dissolution profiles (mean \pm standard deviation, $n=3$) of granules in sachet (filled circle), granules for compression of 120 mg film-coated tablets (empty triangle), final blend for compression of 120 mg film-coated tablets (empty diamond), and film-coated tablet (filled square) in FeSSIF pH 5

the model performance obtained from the Loo-Riegelmann and the numerical deconvolution method was comparatively

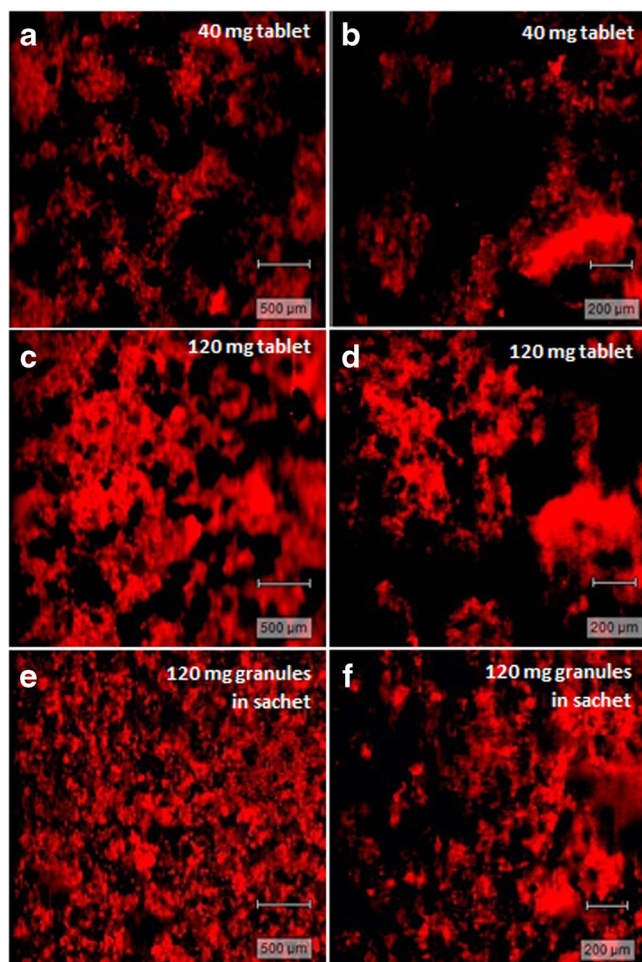


Fig. 6. Raman images of 40 mg tablets (a, b), 120 mg film-coated tablets (c, d), and 120 mg granules in sachet formulation (e, f). Each formulation is shown in two different magnifications. Basmisanil is marked in red and the tablet matrix in black

poor with R^2 values smaller than 0.90. The individual R^2 , SEP, MAE, and AIC values for different deconvolution methods are reported in the [Supplementary Material](#).

Validation of the IVIVC model was conducted with the plasma concentration-time profiles obtained following administration of 0.5 to 1250 mg as tablet formulation (MAD and SAD study data). The model provided a good prediction of oral exposure over the entire dose range, as shown in Fig. 8. The plasma concentration-time profiles, which were predicted using the IVIVC model, were included in the [Supplementary Material](#).

DISCUSSION

Understanding the mechanism of drug liberation, dissolution, and absorption from the gastrointestinal tract is of key importance for the development of high quality drug products. In the present study, we investigated the rate-limiting processes for oral absorption of the poorly water-soluble compound Basmisanil and the difference in exposure between two formulations by means of oral absorption modelling and dissolution testing.

The oral absorption model developed using GastroPlus was in most of the cases well predictive for *in vivo* exposure over a large dose range. However, some discrepancy was observed depending on the formulation. The model prediction was comparatively poor for the 120-mg film-coated tablet data, which exhibited lower peak plasma concentrations compared to the granules formulation, even though the same dose of 120 mg was administered (Fig. 1b). This observation suggested that there was an underlying difference in release kinetics between the two dosage forms, which was further investigated.

SAD and MAD study data showed a dose proportional increase in C_{max} and AUC in the dose range from 1.5 to approximately 160 mg, but less than proportional exposure for higher doses (Fig. 1a). The GastroPlus model resulted in an excellent prediction of this non-linearity, particularly with regard to C_{max} (Fig. 2a). It was therefore reasonable to explore the mechanism of this dose-dependent exposure by means of oral absorption modelling.

The particle size of Basmisanil was found to be a critical parameter with regard to drug absorption (Fig. 3). The simulated intraluminal dissolution profiles of small, medium, and large drug particles suggested an initial dissolution rate-limited drug release, followed by a saturation effect of intestinal fluids during later intestinal transit. Based on FeSSIF solubility data, the 1.5-mg drug dose can be assumed to be completely soluble in the fed state intestine. Therefore, drug absorption was likely limited by the dissolution rate only. At higher dose levels, however, the concentration of dissolved Basmisanil approached the solubility limit in intestinal fluids. Drug release and absorption were initially dissolution rate limited, but became solubility-limited following solubilisation of the small particles fraction. This effect could explain the drop in dissolution during intestinal transit as well as the incomplete drug absorption observed at higher doses.

The findings on the rate-limiting processes in oral absorption of Basmisanil indicated potential root causes for the difference in exposure between the granules and the film-

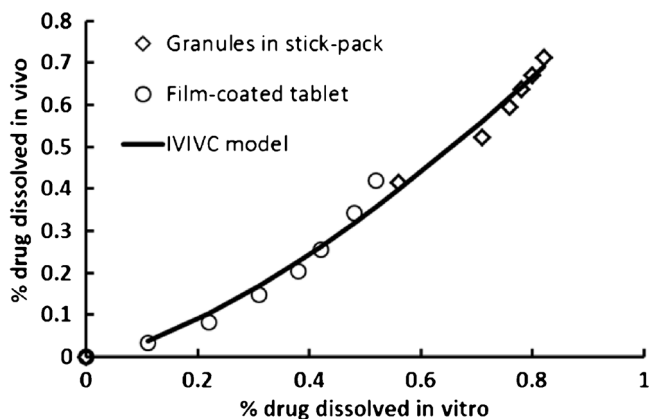


Fig. 7. Correlation between *in vitro* and *in vivo* dissolution data obtained following deconvolution of *in vivo* profiles using the GastroPlus Mechanistic Absorption Model. The data were best fitted by a power correlation function

coated tablet formulation. These two formulations were administered at single doses of 120 mg and, at this dose, oral exposure was shown to be particularly sensitive towards particle size (Fig. 3). Minor changes in API and/or formulation properties may therefore influence the drug release behaviour and the rate of absorption.

To investigate the formulation properties and their impact on drug release, we conducted *in vitro* dissolution studies in FeSSiF and Raman imaging. The *in vitro* dissolution method captured a difference in drug release between the granules in sachets and the film-coated tablet. Tablet compression had some influence on the kinetics of dissolution, which was in good agreement with previous findings (19). However, a significant difference was observed between the dissolution rate of the granules for tablet compression and the granules in sachet formulation. Considering that the qualitative composition and the manufacturing technology (roll compaction) of the two granules were identical and the two formulations only differed in drug load (12.8 vs. 34.2% w/w), this formulation property was supposed to be the root cause for the difference in dissolution behaviour and *in vivo*

plasma profiles between formulations. The percolation theory describes the formation of clusters in a random system. In a binary powder system consisting of components A and B, the particles of component A form isolated clusters within a continuous phase of the component B below a critical concentration that is referred to as the percolation threshold. Once the percolation threshold of component A is exceeded, these particles form a coherent network (infinite cluster) and dominate the characteristics of the whole system (20–23).

Raman images evidenced that the micronized primary API particles were not dispersed as single particles in the tablet, but formed large agglomerated clusters that percolated the hydrophilic tablet matrix. It is reasonable to assume that, after tablet disintegration, the agglomeration of micronized API particles resulted in the release of large clusters instead of micronized primary particles (24). This observation was in line with the results of parameter sensitivity analysis.

Drug particle agglomeration could be attributed to the fact that the manufacturing process involved two unit operations, which were both based on densification *via* pressure, *i.e.* roll compaction and tablet compression. Additionally, increasing the drug load resulted in a higher drug-excipient ratio in the solid formulation, which facilitated the agglomeration of drug particles. The results of parameter sensitivity analysis, *in vitro* dissolution studies, and Raman imaging allowed the conclusion that the critical concentration of the poorly soluble API was exceeded in the 120-mg film-coated tablet formulation which was likely the root cause of the difference in dissolution behaviour and the discrepancy that was observed during pharmacokinetic modelling for this formulation.

In the dose range below approx. 160 mg Basimisanil, the GastroPlus model resulted in an accurate prediction of oral exposure for those formulations which released primary drug particles following disintegration (*i.e.* drug load below percolation threshold). In this case, the absorption rate was mainly driven by the dissolution rate of primary particles. The simulation was however comparatively poor when clustering of micronized API particles occurred during powder compression, as shown for the film-coated tablet. In those

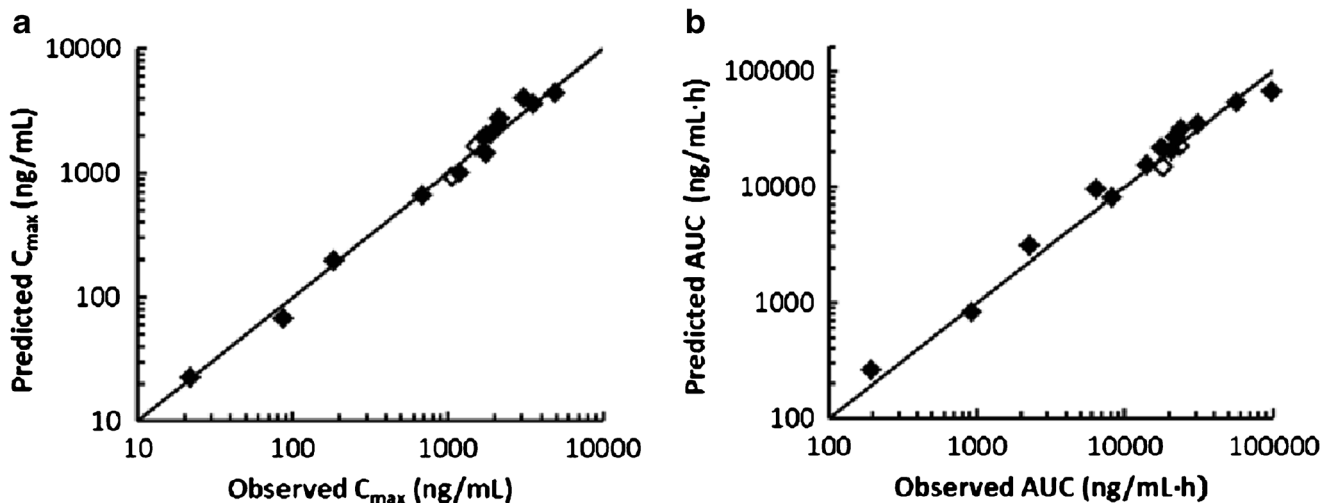


Fig. 8. Observed *versus* predicted **a** C_{max} and **b** AUC values resulting from the IVIVC model developed using the GastroPlus mechanistic absorption model as deconvolution method and by fitting a double Weibull function to the *in vivo* dissolution data. The *open symbols* represent the two datasets used for IVIVC model development

situations, the establishment of an IVIVC model provides clear advantages for predicting oral exposure, as it captures the release properties of the entire formulation including the influence of excipients and process parameters on the release profile.

In the present study we compared the suitability of the Loo-Riegelmann, the numerical deconvolution, and the GastroPlus Mechanistic Absorption model as deconvolution methods for modelling the *in vivo* dissolution profiles of Basmisanil. The GastroPlus Mechanistic Absorption method was superior to the traditional deconvolution methods. An excellent correlation was obtained between deconvoluted *in vivo* dissolution profiles and the *in vitro* dissolution data in FeSSIF. This deconvolution process considers the full Advanced Compartmental Absorption and Transit (ACAT) model and, in general, it allows modelling of complex (pre-)absorption processes such as regionally dependent absorption, pH-dependent solubility, precipitation, influx and efflux transport, food effect, and saturable kinetics. This is different from the traditional and comparatively simple Loo-Riegelmann or numerical deconvolution, which are typically used for IVIVCs in the fasted state. These methods were shown to be suitable for compounds with linear and non-saturable absorption kinetics that are well-absorbed throughout the GI tract (25–27). In the case of Basmisanil, however, the kinetics of drug absorption is dissolution rate and solubility-limited, depending on the dose, and is influenced by the fed state physiology (e.g. prolonged gastric emptying time), in which case the GastroPlus Mechanistic Absorption method provided a clear benefit.

CONCLUSIONS

The present study evidences the strengths of combined absorption modelling and *in vitro* dissolution testing to elucidate the rate-limiting steps of oral drug absorption. These tools were applied to explain the difference in oral systemic exposure between two immediate-release formulations containing a BCS class 2 compound. The drug load of a poorly water-soluble and micronized API was shown to have a critical impact on the dissolution rate and *in vivo* performance of solid dosage forms which were manufactured *via* roll compaction. Moreover, an IVIVC model was developed which supports future formulation development as a link between formulation properties and *in vivo* formulation performance. In case of Basmisanil, which undergoes dose-dependent dissolution- and solubility-limited absorption and which was administered in the fed state, the use of a mechanistic deconvolution method provided a clear benefit in terms of IVIVC model performance.

Such advanced understanding of *in vivo* formulation performance is important for a rational and science-driven development of oral formulations according to the QbD strategy. The study finally illustrates the validity and applicability of biopharmaceutical *in vitro* and *in silico* tools and demonstrates their potential during drug development.

ACKNOWLEDGEMENTS

The authors would like to thank Dr. Anni Pabst-Ravot (F. Hoffmann-La Roche Ltd., Basel, Switzerland) for analytical

support. Dr. Carsten Brüsewitz (F. Hoffmann-La Roche Ltd., Basel, Switzerland) is gratefully acknowledged for providing the clinical study material for pharmacokinetic studies.

REFERENCES

1. FDA. Guidance for Industry Q8(R2) Pharmaceutical Development. FDA (CDER). 2009.
2. Polli JE, Cook JA, Davit BM, Dickinson PA, Argenti D, Barbour N, *et al.* Summary workshop report: facilitating oral product development and reducing regulatory burden through novel approaches to assess bioavailability/bioequivalence. *AAPS J.* 2012;14(3):627–38. doi:10.1208/s12248-012-9376-z.
3. Kesisoglou F, Rossenu S, Farrell C, Van Den Heuvel M, Prohn M, Fitzpatrick S, *et al.* Development of *in vitro*-*in vivo* correlation for extended-release niacin after administration of hypromellose-based matrix formulations to healthy volunteers. *J Pharm Sci.* 2014;103(11):3713–23. doi:10.1002/jps.24179.
4. Eaga C, Mantri S, Malayandi R, Kondamudi PK, Chakraborty S, Raju SVN, *et al.* Establishing postprandial bio-equivalency and IVIVC for generic metformin sustained release small sized tablets. *J Pharm Investig.* 2014;44(3):197–204. doi:10.1007/s40005-013-0115-y.
5. Ilic M, Duris J, Kovacevic I, Ibric S, Parojcic J. *In vitro*-*in silico*-*in vivo* drug absorption model development based on mechanistic gastrointestinal simulation and artificial neural networks: nifedipine osmotic release tablets case study. *Eur J Pharm Sci.* 2014;62:212–8. doi:10.1016/j.ejps.2014.05.030.
6. Parejiya PB, Barot BS, Patel HK, Chorawala MR, Shelat PK, Shukla A. *In vivo* performance evaluation and establishment of IVIVC for osmotic pump based extended release formulation of milnacipran HCl. *Biopharm Drug Dispos.* 2013;34(4):227–35. doi:10.1002/bdd.1840.
7. Selen A, Cruaños M, Müllertz A, Dickinson P, Cook J, Polli J, *et al.* Meeting report: applied biopharmaceutics and quality by design for dissolution/release specification setting: product quality for patient benefit. *AAPS J.* 2010;12(3):465–72. doi:10.1208/s12248-010-9206-0.
8. Zhang X, Lionberger RA, Davit BM, Yu LX. Utility of physiologically based absorption modeling in implementing Quality by Design in drug development. *AAPS J.* 2011;13(1):59–71. doi:10.1208/s12248-010-9250-9.
9. Kesisoglou F, Mitra A. Application of absorption modeling in rational design of drug product under Quality-by-Design paradigm. *AAPS J.* 2015;17(5):1224–36. doi:10.1208/s12248-015-9781-1.
10. Mathias NR, Crison J. The use of modeling tools to drive efficient oral product design. *AAPS J.* 2012;14(3):591–600. doi:10.1208/s12248-012-9372-3.
11. Zhang H, Xia B, Sheng J, Heimbach T, Lin T-H, He H, *et al.* Application of physiologically based absorption modeling to formulation development of a low solubility, low permeability weak base: mechanistic investigation of food effect. *AAPS PharmSciTech.* 2014;15(2):400–6. doi:10.1208/s12249-014-0075-1.
12. Flanagan T, Van Peer A, Lindahl A. Use of physiologically relevant biopharmaceutics tools within the pharmaceutical industry and in regulatory sciences: where are we now and what are the gaps? *Eur J Pharm Sci.* 2016;91:84–90. doi:10.1016/j.ejps.2016.06.006.
13. Johnson KC, Swindell AC. Guidance in the setting of drug particle size specifications to minimize variability in absorption. *Pharm Res.* 1996;13(12):1795–8. doi:10.1023/a:1016068705255.
14. Galia E, Nicolaidis E, Hörter D, Löbenberg R, Reppas C, Dressman JB. Evaluation of various dissolution media for predicting *in vivo* performance of class I and II drugs. *Pharm Res.* 1998;15(5):698–705. doi:10.1023/a:1011910801212.
15. Parrott N, Lave T. Applications of physiologically based absorption models in drug discovery and development. *Mol Pharm.* 2008;5(5):760–75. doi:10.1021/mp8000155.

16. Wagner JG. Pharmacokinetic absorption plots from oral data alone or oral/intravenous data and an exact Loo–Riegelman equation. *J Pharm Sci.* 1983;72(7):838–42. doi:10.1002/jps.2600720738.
17. Langenbucher F. Handling of computational in vitro/in vivo correlation problems by Microsoft Excel: III. Convolution and deconvolution. *Eur J Pharm Biopharm.* 2003;56(3):429–37. doi:10.1016/S0939-6411(03)00140-1.
18. Kostewicz ES, Aarons L, Bergstrand M, Bolger MB, Galetin A, Hatley O, *et al.* PBPK models for the prediction of in vivo performance of oral dosage forms. *Eur J Pharm Sci.* 2014;57:300–21. doi:10.1016/j.ejps.2013.09.008.
19. Potharaju S. Effect of compression force on agglomeration of micronized active pharmaceutical ingredients: techniques to prevent API agglomeration during compression. Tennessee: University of Tennessee Health Science Center; 2012.
20. Leuenberger H. The application of percolation theory in powder technology. *Adv Powder Technol.* 1999;10(4):323–52. doi:10.1163/156855299X00190.
21. Mohamed FA, Roberts M, Seton L, Ford JL, Levina M, Rajabi-Siahboomi AR. The effect of HPMC particle size on the drug release rate and the percolation threshold in extended-release mini-tablets. *Drug Dev Ind Pharm.* 2015;41(1):70–8. doi:10.3109/03639045.2013.845843.
22. Miranda A, Millan M, Caraballo I. Investigation of the influence of particle size on the excipient percolation thresholds of HPMC hydrophilic matrix tablets. *J Pharm Sci.* 2007;96(10):2746–56. doi:10.1002/jps.20912.
23. Boersen N, Carvajal MT, Morris KR, Peck GE, Pinal R. The influence of API concentration on the roller compaction process: modeling and prediction of the post compacted ribbon, granule and tablet properties using multivariate data analysis. *Drug Dev Ind Pharm.* 2015;41(9):1470–8. doi:10.3109/03639045.2014.958754.
24. Hirschorn JO, Kornblum SS. Dissolution of poorly water-soluble drugs II: excipient dilution and force of compression effects on tablets of a quinazolinone compound. *J Pharm Sci.* 1971;60(3):445–8. doi:10.1002/jps.2600600321.
25. Honório da Silva T, Pinto EC, Rocha HVA, Esteves VSAD, dos Santos TC, Castro HCR, *et al.* In vitro–in vivo correlation of Efavirenz tablets using GastroPlus®. *AAPS PharmSciTech.* 2013;14(3):1244–54. doi:10.1208/s12249-013-0016-4.
26. Kesisoglou F, Xia B, Agrawal NGB. Comparison of deconvolution-based and absorption modeling IVIVC for extended release formulations of a BCS III drug development candidate. *AAPS J.* 2015;17(6):1492–500. doi:10.1208/s12248-015-9816-7.
27. Margolskee A, Darwich AS, Galetin A, Rostami-Hodjegan A, Aarons L. Deconvolution and IVIVC: exploring the role of rate-limiting conditions. *AAPS J.* 2016;18(2):321–32. doi:10.1208/s12248-015-9849-y.